 doi:10.20944/preprints202204.0229.v1

Article

Thermodynamic Study of Solar Assisted Hybrid Cooling Systems With Consideration of Duration in Heat-Driven Processes

Zeyu Peng [1,2,3], Zeyu Li [1,2,3,*], Junquan Zeng [1,2,3] and Jianting Yu [4]

[1] School of Electric Power, South China University of Technology, Guangzhou 510640, China
[2] Guangdong Province Key Laboratory of High Efficient and Clean Energy Utilization, South China University of Technology, Guangzhou 510640, China
[3] Guangdong Province Engineering Research Center of High Efficient and Low pollution Energy Conversion, Guangzhou 510640, China
[4] Shenzhen Engineering Research Centre for Gas Distribution and Efficient Utilization, Shenzhen Gas Corporation Ltd., Shenzhen 518049, China
* Correspondence: epzeyuli@scut.edu.cn; Tel: +86-20-87110213

Abstract: Solar assisted hybrid cooling systems are promising for the energy saving of refrigeration systems. In most cases, the solar thermal gain is only able to power the heat-driven process of facilities in part of the working period. Therefore, the reduction of compressor power strongly depends upon the duration of heat-driven processes, which has not been addressed properly. Motivated by such knowledge gap, the thermodynamic understanding of solar assisted hybrid cooling systems is deepened through considering the duration in heat-driven processes. Three absorption-compression integrated cooling cycles were taken as examples. It is found that optimal parameters, e.g., inter-stage pressure and temperature, corresponding to various performance indicators trend to be identical, as the duration of heat-driven processes is taken into account. Furthermore, the optimal parameter for different working conditions was obtained. It is displayed that the dimensionless optimal intermediate temperature of layout with the cascade condensation process varies slightly, e.g., 4%, for different conditions. Moreover, the fall of compressor power in entire working periods is nearly independent upon the intermediate temperature. The paper is favorable for the efficient design and operation of solar assisted hybrid cooling systems.

Keywords: Solar energy; Refrigeration; Absorption-compression; Energy saving; Thermodynamic model

Nomenclature

Abbreviations		ψ	heat powered coefficient of performance
Exp	experimental	η	efficiency, effectiveness, energy saving factor
GWP	global warming potential	*Subscripts*	
LCC	layout with cascade condensation process	a	absorber
LCS	layout with cascade subcooling process	as	absorption subsystem
Th	theoretical	c	condenser

 doi:10.20944/preprints202204.0229.v1

TSCTMC	two-stage cycle with thermal and mechanical compression processes	ca	chilled air
Symbols		com	compressor
COP	coefficient of performance	cw	cooling water
ECOP	exergy efficiency	e	evaporator
ex	specific exergy (kJ/kg)	g	generator
Ex	exergy rate (kW)	hs	hybrid cooling system
h	specific enthalpy (kJ/kg)	hw	hot water
m	mass flow rate (kg/s)	in	inlet
Q	energy (kW)	int	inter-stage
Q_h	heat quantity (kW)	is	isentropic
T	temperature (K)	m	intermediate
W	work (kW)	opt	optimum
X	concentration	out	outlet
Greek		pump	pump
Δ	difference	ref	reference
α	dimensionless optimum intermediate temperature	shx	solution heat exchanger
β	dimensionless optimum inter-stage pressure	tot	total
γ	duration in heat-driven processes		

1. Introduction

Refrigeration systems are responsible for more than 60% of the total energy consumption in buildings [1] and around 11% of the worldwide annual electricity consumption in cold chain industries [2]. Consequently, the reduction in refrigeration consumption is essential, especially under the background of carbon neutralization. Solar cooling technologies are promising to reduce the consumption of refrigeration systems, because the solar energy is clean, abundant, and coincident to the cooling demand. Among various solar cooling technologies, solar assisted hybrid cooling systems based on the absorption-compression integrated cycle serve as the potential solution in replacing traditional electric-driven chillers, owing to the consideration of performance and reliability.

There are generally three solar assisted hybrid cooling systems based on the absorption-compression integrated cycle, e.g., two-stage cycle with thermal and mechanical compression processes and layout with cascade condensation process for industry cooling as well as layout with cascade subcooling process for building cooling. The corresponding thermodynamic studies are reviewed in the following subsection.

1.1. Two-stage cycle with thermal and mechanical compression processes

Two-stage cycle with thermal and mechanical compression processes is derived from the traditional two-stage compression cycle, in which one of the mechanical compression processes is replaced by the thermal one. Note that only the layout in which the thermal compression locates at the high-pressure stage is taken into account, since its performance

Preprints (www.preprints.org) | NOT PEER-REVIEWED | Posted: 26 April 2022 doi:10.20944/preprints202204.0229.v1

is more than another configuration [3]. The literature reviews are summarized in Table 1. It was found that the optimum inter-stage pressure for heat powered coefficient of performance (ψ) as well as electricity saving rate varied from 250 kPa to 900 kPa for different working conditions [4]. Furthermore, the maximum energy saving rate can be 10–20% higher than that of absorption heat pump [5] and 45.16–65.74% greater than that of compression system [6], respectively. The heating *COP* was around 1.103 to 1.511 for different working conditions [7], and was 4.6–69.54% greater than that of varieties of heat pumps [8,9]. Moreover, the maximum heating exergy efficiency (*ECOP*) was around 0.55–0.68 for different working substances [10]. In addition, the maximal cooling *COP* and *ECOP* of hybrid system were around 1.4–4 [11,12] and 2–3 times [13] that of absorption chiller, respectively.

Table 1. Summary of literature survey on two-stage cycle with thermal and mechanical compression processes.

Ref.	Th./Exp. study	Working fluid	Main findings
[14]	Th.	R134a/DMF	The optimal inter-stage pressure for ψ varied from 300 kPa to 750 kPa in different working conditions.
[4]	Th.		The optimal inter-stage pressure for ψ and electricity saving rate varied from 300 kPa to 900 kPa and 250 kPa to 850 kPa, respectively in different working conditions.
[5]	Exp.	NH_3/H_2O	The maximum energy saving rate can be 10–20% higher than that of absorption heat pump.
[7]	Exp.		The heating *COP* changed from 1.103 to 1.511 in different working conditions.
[8]	Th.		The heating *COP* of hybrid system was 16.35–40.08% and 50.07–69.54% more than that of water and air source heat pump, respectively.
[9]	Exp.		The heating *COP* for hybrid system was 4.6–26.7% higher than that for absorption system.
[10]	Th.	Low GWP refrigerants/ ionic liquid	The maximum heating *ECOP* was around 0.55–0.68 for different working substances.
[11]	Th.		The maximal *COP* of hybrid cooling system was 1.4–1.9 times that of absorption chiller.
[12]	Th.		The cooling *COP* of hybrid system was more than 4 times that of absorption refrigeration system.
[13]	Th.		The maximal cooling *ECOP* of hybrid system was around 2–3 times that of absorption chiller.
[6]	Th.		The electricity consumption of hybrid system was decreased by 45.16–65.74%, compared with compression system.
[15]	Th.		The maximum cooling *COP* of hybrid system with R1234yf/[hmim][Tf_2N] was 75% higher than that with R1234yf/[hmim][TfO].

1.2. Layout with cascade condensation process

Layout with cascade condensation process is also derived from the traditional two-stage compression cycle. Such system consists of absorption and compression refrigeration subcycle, and the evaporation process of absorption subcycle (high temperature stage) is coupled with the condensation one of compression cycle (low temperature stage). Thermodynamic studies on layout with cascade condensation process are exhibited in Table 2. It was displayed that the performance of compression subsystem of layout with cascade condensation process has been highly enhanced. For example, the *COP* of compression section was improved by 37–155% [16,17] and the electricity consumption was decreased by 26.7–73% [18,19]. Furthermore, the global *COP* of hybrid system can be increased by 25.4% [20].

Table 2. Summary of literature survey on layout with cascade condensation process.

Ref.	Th./Exp. study	Working fluid		Main findings
		Absorption	Compression	
[21]	Exp.	NH_3/H_2O	R22	The electrical energy consumption was decreased by 49.5%.
[22]	Th.	NH_3/H_2O	CO_2, NH_3	*COP* of compression section with CO_2 was enhanced by 5.64%, compared with that with NH_3.
[17]	Th.	NH_3/H_2O	R717, R22, R134a	*COP* of compression subsystems has been increased by 37–54%.
[23]	Th.	LiBr/H_2O	CO_2	31% of electricity demand was reduced.
[24]	Th.	LiBr/H_2O	CO_2	Cooling capacity was grown by 74.4% when taking double-effect absorption chiller as absorption subsystem.
[25]	Th.	NH_3/H_2O, LiBr/H_2O	R134a, R410A, NH_3	Electrical energy consumption was decreased by 48–51%.
[19]	Th.	NH_3/H_2O, LiBr/H_2O	R134a, R410A, NH_3	Power consumption was decreased by 73% for system with double-effect absorption subsystem.

Preprints (www.preprints.org) | NOT PEER-REVIEWED | Posted: 26 April 2022 doi:10.20944/preprints202204.0229.v1

[26]	Th.	LiBr/H_2O	R1234yf	Layout with triple-effect absorption subcycle saved 45.84% of electricity.
[16]	Th.	LiBr/H_2O	R22, R134a, R410A, R407C	Electric power consumption was reduced by 61% and *COP* of the compression section was improved by 155%.
[27]	Th.	NH_3/H_2O	CO_2	Primary energy consumption was reduced by 60.6% and electrical *COP* was improved by 153.6%.
[28]	Th.	LiBr/H_2O	R22	The evaporator and condenser fouling resulted in 9.22% of reduction in energy saving amount.
[29]	Th.	LiBr/H_2O, LiCl/H_2O	R1234yf, R1234ze(E), R1233zd(E)	The electricity consumption was decreased 51.36–54.16%.
[30]	Th.	LiBr/H_2O	R134a, CO_2	*COP* for system adopting double-effect absorption subsystem could be grown by around 50%.
[20]	Th.	LiBr/H_2O	R134a	When detailed condition optimization was considered, the global *COP* in different cases was enhanced by 25.4% and 6.7%, respectively.
[18]	Th.	LiBr/H_2O	R134a	26.7% of power consumption was avoided on the whole cooling season.

1.3. Layout with cascade subcooling process

Layout with cascade subcooling process mainly serves as the energy saving layout of traditional vapour compression chillers in building cooling. It also composes of absorption and compression refrigeration cycle, and the evaporation process of absorption subcycle is coupled with the subcooling one of compression subcycle. Literature survey on layout with cascade subcooling process is summarized in Table 3. It was exhibited that the energy saving rate for layout with cascade subcooling process was around 7.67% to 35% [31,32]. Moreover, the exergy efficiency was increased by 26.9%, as compared with compression system [33]. In addition, the subcooling power cannot be fully converted into cooling output enhancement in the constant superheating condition [34]. Nevertheless, in the case of fixed opening mode of throttling valve, the enhanced cooling capacity can exceed the subcooling power [35].

Table 3. Summary of literature survey on cooling systems with cascade subcooling process.

Ref.	Th./Exp. study	Working fluid		Main findings
		Absorption	Compression	
[33]	**Th.**	LiBr/H_2O	CO_2	Overall *COP* as well as exergy efficiency *ECOP* increased by 28.6% and 26.9%, respectively.
[32]	Th.	LiBr/H_2O, NH_3/H_2O	R134a	Energy consumption decreased by 24% and 35%, respectively when taking LiBr/H_2O and NH_3/H_2O chiller.
[36]	Th./Exp.	LiBr/H_2O	R22	Cooling capacity was increased by around 37.8%, as subcooling power enhanced by 33.3%.
[31]	Th.	LiBr/H_2O	R410A	Maximum energy saving fraction increased from 7.67% to 11.0% on whole cooling season.
[37]	Exp.	LiBr/H_2O	R410A	Compressor work reduced by 13–22% in different typical day.
[38]	Th.	LiBr/H_2O	NH_3	System with the cool energy buffer excluding the shift of solar cooling power saved 11.4% of compressor work.
[34]	Th.	LiBr/H_2O	R410A	Subcooling power cannot be fully converted into an increase of the cooling capacity in the constant superheating condition.
[35]	Exp.	LiBr/H_2O	R410A	Enhanced cooling capacity can exceed the subcooling power in the fixed opening mode of throttling valve.

1.4. Knowledge gap and aim of this work

Remarkable energy saving of three representative layouts emerges according to the existing study. Furthermore, their performances strongly depend upon critical parameters, i.e., there is an optimal cascade temperature maximizing performance indicators for cascade layouts. In this regard, parameters of the inter-stage/cascade process should be designed exactly in terms of operation characteristics for solar assisted

hybrid cooling systems, which have not been addressed properly in the open literature. The corresponding limitation lies in the following aspects:

(1) The duration of heat-driven processes is not taken into account in the impact of the inter-stage/cascade parameters. Because collectors are usually installed in the roof of buildings, the relatively insufficient collector area and solar thermal gain are incapable to maintain the duration of heat-driven processes in entire working periods. When the solar thermal gain is exhausted, solar assisted hybrid cooling systems are degraded to electric-driven chillers with null energy saving. Therefore, it can be implied that the interaction of duration in the heat-driven process, parameters in the inter-stage/cascade process and system performance is strong, i.e., lowering the temperature of cascade condensation process enhances the energy saving and shortens the duration of heat-driven processes simultaneously, leading to the complicated variation of total energy saving in entire working periods.

(2) Optimal parameters of the inter-stage/cascade process corresponding to various performance indicators are conflicting. For example, the optimal intermediate temperature is 10 °C and 7 °C, respectively for the peak global *COP* and energy saving amount in the layout with cascade condensation process [39]. The above-mentioned phenomenon is mainly attributed to the missing consideration of the heat-driven process duration. In this regard, designers are easily subjected to be confused when they attempt to optimize the system.

Motivated by the above-mentioned knowledge gap, we aim to deepen the thermodynamic understanding of solar assisted hybrid cooling systems through considering the duration in heat-driven processes. The remainder of this article is organized as follows. Three representative layouts of solar assisted hybrid cooling systems have been specifically described in Section 2. Thermodynamic modeling is shown in Section 3. The model validation and parameters of case study are presented in Section 4. Analysis for system with sufficient heat input has been exhibited in Section 5.1. The interaction of duration in heat-driven processes, parameters in the inter-stage/cascade process and system performance in the case of insufficient heat input is discussed in Section 5.2. In Section 5.3, optimal parameters for different working conditions are obtained. Finally, the conclusions of this study are summarized in Section 6. The novelty of paper lies in illustrating the relationship of duration in the heat-driven process, parameters of the inter-stage/cascade process and system performance, and obtaining the optimal parameter of the inter-stage/cascade process in entire working periods for solar assisted hybrid cooling systems. The paper is favorable for the development and optimization of solar assisted hybrid cooling systems.

2. System description

Three representative layouts of solar assisted hybrid cooling systems, i.e., two-stage cycle with thermal and mechanical compression processes, hybrid cycle with cascade condensation process and cascade subcooling process, are described briefly in this section.

The schematic diagram of solar assisted two-stage cycle with thermal and mechanical compression processes is exhibited in Figure 1. The cycle is composed of solar collector, cooling tower, compressor, thermal compressor (generator, absorber, solution heat exchanger, solution pump, and throttle valve 2), rectifier, condenser, throttle valve 1 and evaporator. The thermal compressor is driven by the hot pressurized water heated by solar energy. It is demonstrated that the energy saving feature of two-stage cycle with thermal and mechanical compression processes is straightforward, i.e., partial compressor power has been cut down by the heat-driven thermal compressor. Moreover, the energy saving amount of the layout is dependent on the evaporator, condenser, and inter-stage pressure (i.e., outlet pressure of compressor). Note that NH_3/H_2O is chosen as the working fluid for two-stage cycle with thermal and mechanical compression processes, which is attributed to its environmental friendliness and convenience.

Preprints (www.preprints.org) | NOT PEER-REVIEWED | Posted: 26 April 2022 doi:10.20944/preprints202204.0229.v1

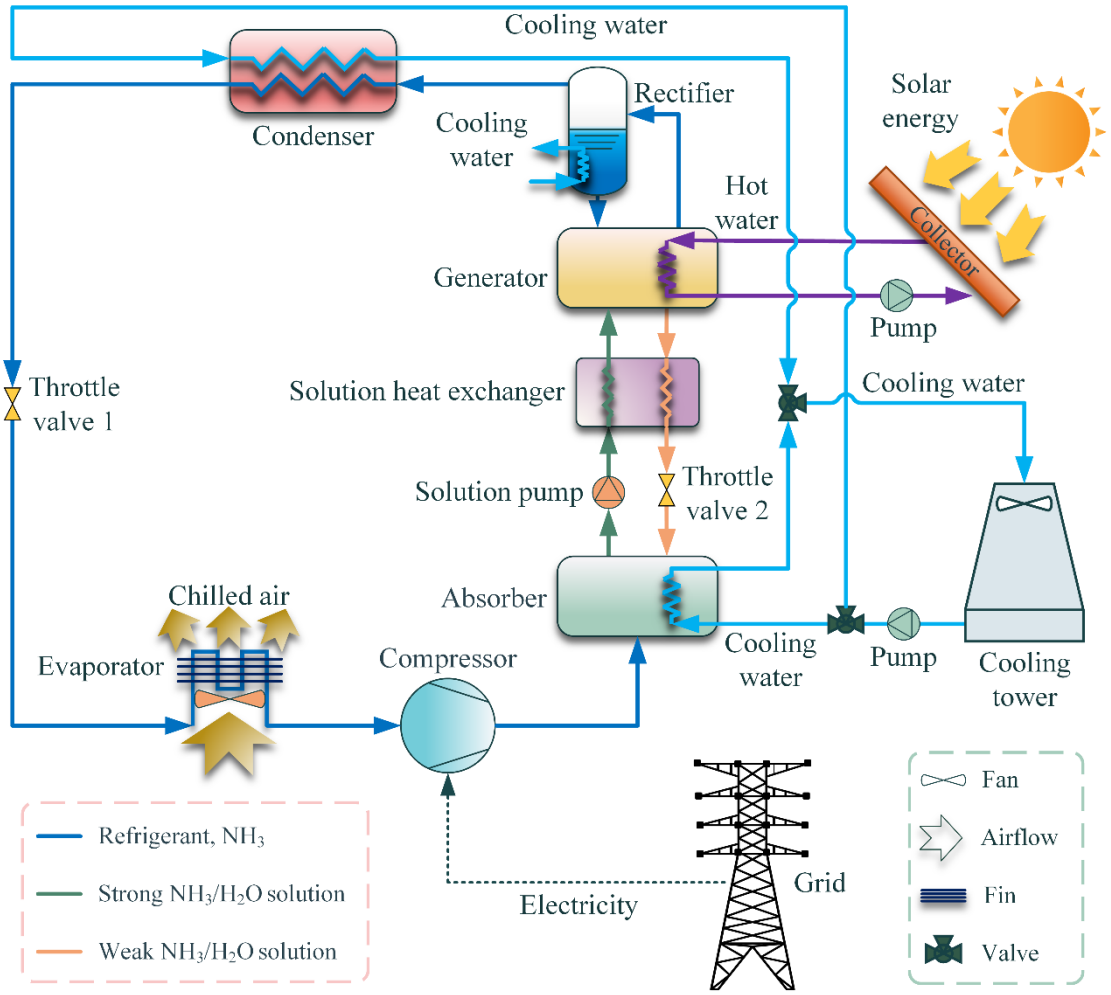

Figure 1. Schematic diagram of solar assisted two-stage cycle with thermal and mechanical compression processes.

The schematic diagram of solar assisted hybrid cooling system with cascade condensation process can be seen in Figure 2. The corresponding system is made up of two subsystems that can be individually operated, i.e., absorption and compression subsystems, which are driven by solar heat and electricity, respectively. The energy saving characteristics of layout with cascade condensation process is that the condenser temperature is decreased, owing to the use of cooling output of absorption subsystems to cool down the condenser of compression one. Accordingly, the energy saving amount of the system is restricted by the evaporator temperature of both compression and absorption subsystems. Specially, the selection of working fluid pairs for layout with condensation process is flexible, because of the independence of the compression and absorption subsystem. In this study, the working fluid of absorption and compression subsystem is selected as $LiBr/H_2O$ and NH_3, respectively. The reason regarding the utilization of $LiBr/H_2O$ absorption chillers lies in its lower temperature of driven heat source and higher *COP* [25].

Preprints (www.preprints.org) | NOT PEER-REVIEWED | Posted: 26 April 2022 doi:10.20944/preprints202204.0229.v1

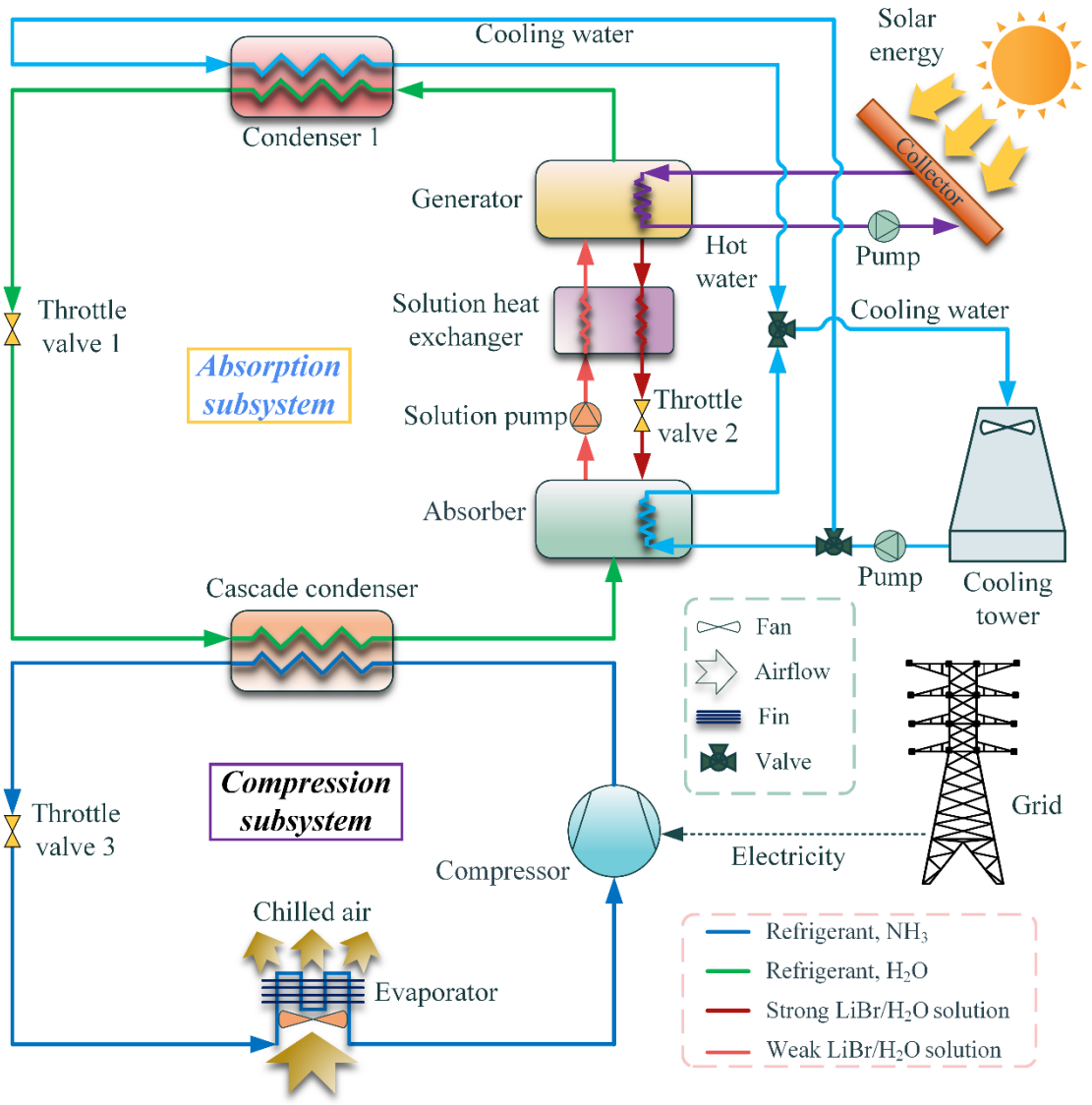

Figure 2. Schematic diagram of solar assisted hybrid cooling system with cascade condensation process.

The schematic diagram of solar assisted hybrid cooling system with cascade subcooling process is displayed in Figure 3. Layout with cascade subcooling process is also composed of absorption and compression subsystems. The energy saving mechanism of the system is that the specific cooling capacity has been enhanced by the subcooling process. Furthermore, the working substance is also chosen as LiBr/H_2O and NH_3, respectively for absorption and compression subsystems.

Preprints (www.preprints.org) | NOT PEER-REVIEWED | Posted: 26 April 2022 doi:10.20944/preprints202204.0229.v1

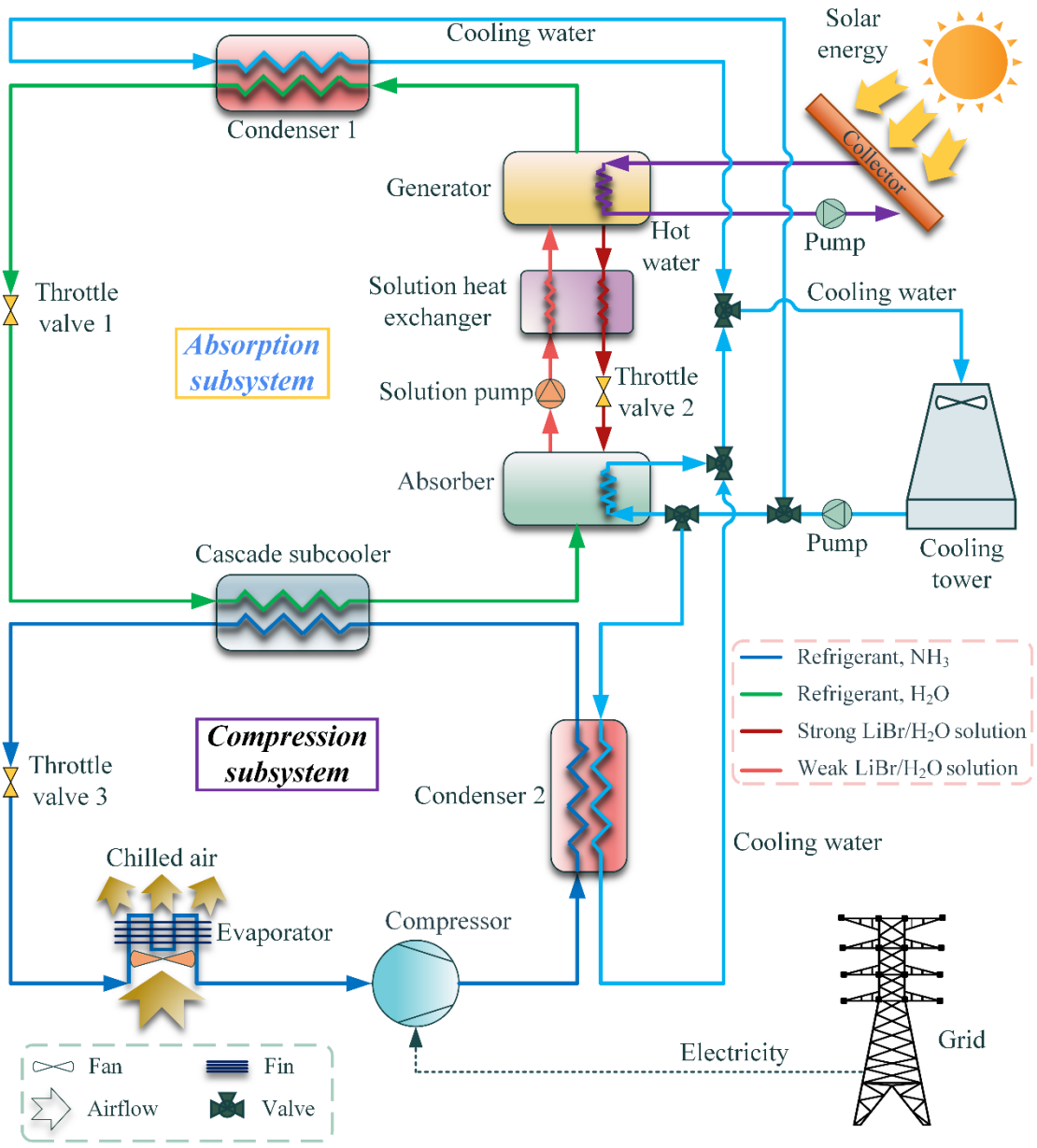

Figure 3. Schematic diagram of solar assisted hybrid cooling system with cascade subcooling process.

Note that the solar assisted hybrid cooling systems will be degraded into traditional vapor compression cycles when the thermal compressor or absorption chillers are switched off, because of the exhaustion of solar heat source.

3. Model

3.1. Assumptions

The thermodynamic models of solar assisted hybrid cooling systems are based on the following assumptions:

1. Systems run under stead conditions [25].
2. Pressure and heat losses are neglected [25].
3. The flows through the throttling devices are isenthalpic, and the solution pump power is neglected [25].
4. Outlets of evaporators and condensers as well as solution outlets of generators and absorbers are saturated [39].

5. The ammonia mass concentration of the refrigerant in two-stage cycle with thermal and mechanical compression processes is 0.998 [40].

6. Dead state temperature and pressure is 25 °C and 100 kPa, respectively. Enthalpy and entropy at the dead state is determined by the pure water properties [41].

The temperature difference between the outlet and inlet of external fluid is fixed at 5 °C. The evaporator temperature of absorption subsystem ($T_{e,as}$) in layout with cascade condensation process and cascade subcooling process and the outlet pressure of compressor in two-stage cycle with thermal and mechanical compression processes is defined as intermediate temperature (T_m) and inter-stage pressure, respectively. The evaporator temperature of solar assisted cooling systems (T_e) is set as $T_{ca,in}-8$; the condenser temperature (T_c) and absorber temperature (T_a) are set as $T_{cw,in}+8$ [42]. The outlet temperature of cascade heat exchangers in the compression side are set as T_m+10 [43]. Additionally, the generator temperature (T_g) is equal to $T_{hw,in}-10$ [44].

3.2. Thermodynamic model

The thermodynamic model of solar assisted cooling systems is analyzed based on the mass, energy and species conservation:

Mass balance, $\sum m=0$ (1)

Energy balance, $\sum Q+\sum W+\sum mh=0$ (2)

Species balance, $\sum mX=0$ (3)

The energy saving amount of solar assisted cooling systems is evaluated by the energy saving factor (η), which is defined as the reduction of compressor power to compressor work of single stage vapor compression system (reference system).

$$\eta=\frac{\Delta W_{tot}}{W_{ref}}=\frac{W_{ref}-W_{com}}{W_{ref}} \quad (4)$$

The exergy efficiency (*ECOP*) of hybrid systems is the total output exergy to the total input exergy.

$$ECOP=\frac{Ex_{out,tot}}{Ex_{in,tot}}=\frac{m_{ca}\left(ex_{ca,out}-ex_{ca,in}\right)}{W_{com}+Ex_{Q_h}} \quad (5)$$

The heat powered coefficient of performance (ψ) introduced in Ref. [14] is utilized to assess the reduction of compressor work per unit of heat source for systems driven by heat and mechanical power, which is redefined based on the exergy viewpoint.

$$\psi=\frac{\Delta W_{tot}}{Ex_{Q_h}} \quad (6)$$

The ψ denotes the efficiency of energy saving with low-grade heat for solar assisted hybrid cooling systems.

Note that the duration in heat-driven processes (γ) should be considered when calculating the compressor work as well as heat exergy for solar assisted hybrid cooling systems with insufficient heat quantity, i.e., heat quantity is less than the heat load of generators.

$$\gamma=\frac{Q_h}{Q_g} \quad (7)$$

The expression of compressor work and heat exergy for solar assisted hybrid cooling systems with sufficient and insufficient heat quantity is listed in Table 4. Note that the

Preprints (www.preprints.org) | NOT PEER-REVIEWED | Posted: 26 April 2022 doi:10.20944/preprints202204.0229.v1

term $W_{ref}-W_{hs}$ represents the specific reduction of compressor power associated with the heat driven process.

Table 4. Expression of compressor work and heat exergy.

Parameter	With sufficient heat source	With insufficient heat source
Compressor work, W_{com}	$W_{com}=W_{hs}$	$W_{com}=\gamma W_{hs}+(1-\gamma)W_{ref}=W_{ref}-\gamma(W_{ref}-W_{hs})$
Heat exergy, Ex_{Q_h}	$Ex_{Q_h}=m_{hw}(ex_{hw,in}-ex_{hw,out})$	$Ex_{Q_h}=\gamma m_{hw}(ex_{hw,in}-ex_{hw,out})$

4. Model validation and case study

Table 5. Comparison of simulation results for two-stage cycle with thermal and mechanical compression processes.

Parameter	Present work	Zhang et al. [3]	Difference
Q_e (MW)	16.92	17	0.47%
Q_g (MW)	24.9	26.08	4.52%
Q_a (MW)	28	28.94	3.25%
Q_c (MW)	18.01	17.64	2.10%
W_{pump} (MW)	0.234	0.245	4.49%
W_{com} (MW)	3.267	3.245	0.68%
COP	0.503	0.488	3.07%

The thermodynamic models of layout with cascade condensation process and layout with cascade subcooling process have been validated in our previous study [45], respectively according to Ref. [25] and [39]. Good agreements are obtained. Moreover, the comparative parameters of two-stage cycle with thermal and mechanical compression processes are calculated according to the thermodynamic properties listed in Ref. [3]. As displayed in Table 5, the maximum relative error is less than 5%.

A case study with respect to the parametric analysis of proposed thermodynamic model is carried out. The corresponding design condition of related systems is shown in Table 6. Two cases, i.e., the heat quantity is equal to the heat load of generators (case 1, also known as the case of sufficient heat input) and is insufficient for the entire working period (case 2), are considered. That is, case 2 is related to the thermodynamic model with consideration of duration in heat-driven processes. Note that the layout with cascade subcooling process is suitable for the small scale heat source, therefore, the heat quantity is much smaller than that of two-stage cycle with thermal and mechanical compression processes and layout with cascade condensation process. The thermodynamic model is solved by the MATLAB program. The thermodynamic property of LiBr/H_2O solution is calculated according to Patek and Klomfar [46]. Additionally, the thermodynamic properties of NH_3 and H_2O are obtained by means of REFPROP 9.1 software.

Table 6. Design and working conditions of the case study.

System	Parameter	Value	
		Case 1	Case 2
TSCTMC	Inlet temperature of hot water, $T_{hw,in}$ (°C)	120	
	Inlet temperature of chilled air, $T_{ca,in}$ (°C)	-10	
	Heat quantity, Q_h (kW)	Heat load of generator	50
LCC	Inlet temperature of hot water, $T_{hw,in}$ (°C)	80	
	Inlet temperature of chilled air, $T_{ca,in}$ (°C)	-10	
	Heat quantity, Q_h (kW)	Heat load of generator	50
LCS	Inlet temperature of hot water, $T_{hw,in}$ (°C)	80	
	Inlet temperature of chilled air, $T_{ca,in}$ (°C)	10	
	Heat quantity, Q_h (kW)	Heat load of generator	2
	Inlet temperature of cooling water, $T_{cw,in}$ (°C)	27	
	Effectiveness of solution heat exchanger, η_{shx}	0.7	
	Isentropic efficiency of compressor, η_{is}	0.7	
	Cooling capacity, Q_e (kW)	100	

5. Results and discussion

Preprints (www.preprints.org) | NOT PEER-REVIEWED | Posted: 26 April 2022 doi:10.20944/preprints202204.0229.v1

There are three parts in this section: (1) system under sufficient heat input, (2) system under insufficient heat input, and (3) optimum parameters for different working conditions.

5.1. System under sufficient heat input

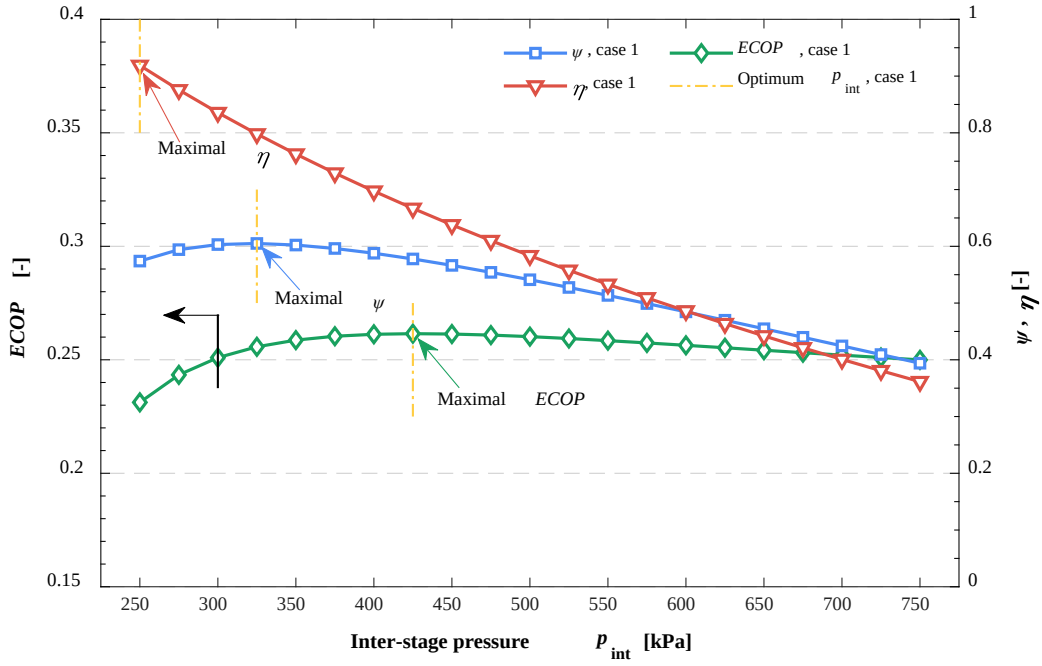

Figure 4. Effect of inter-stage pressure on performance indicators for two-stage cycle with thermal and mechanical compression processes in the case 1.

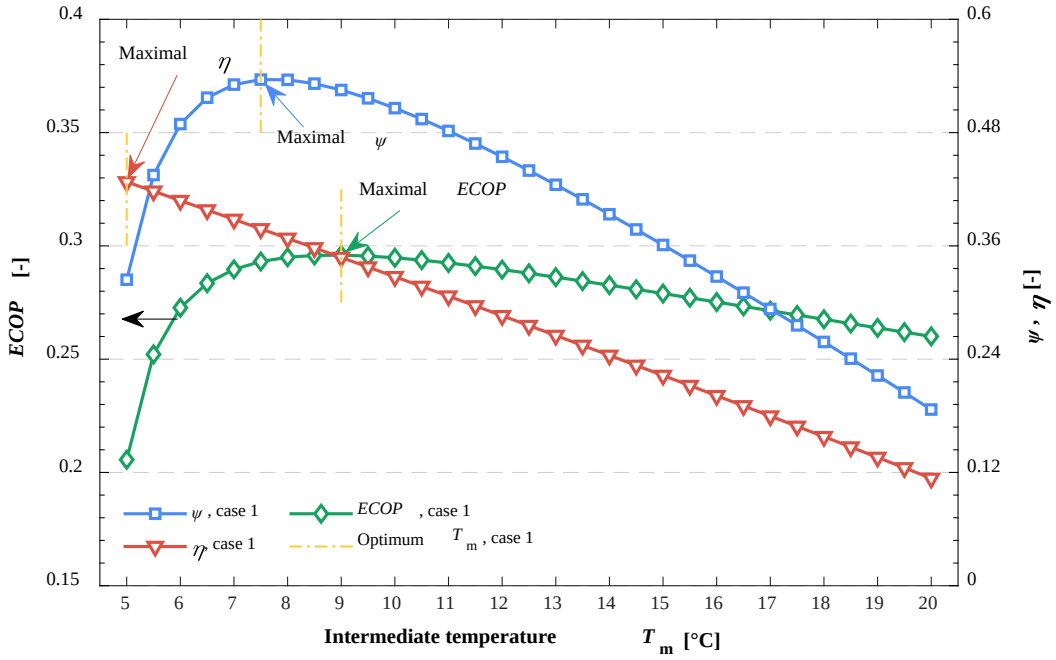

Figure 5. Effect of intermediate temperature on performance indicators for layout with cascade

Preprints (www.preprints.org) | NOT PEER-REVIEWED | Posted: 26 April 2022 doi:10.20944/preprints202204.0229.v1

condensation process in the case 1.

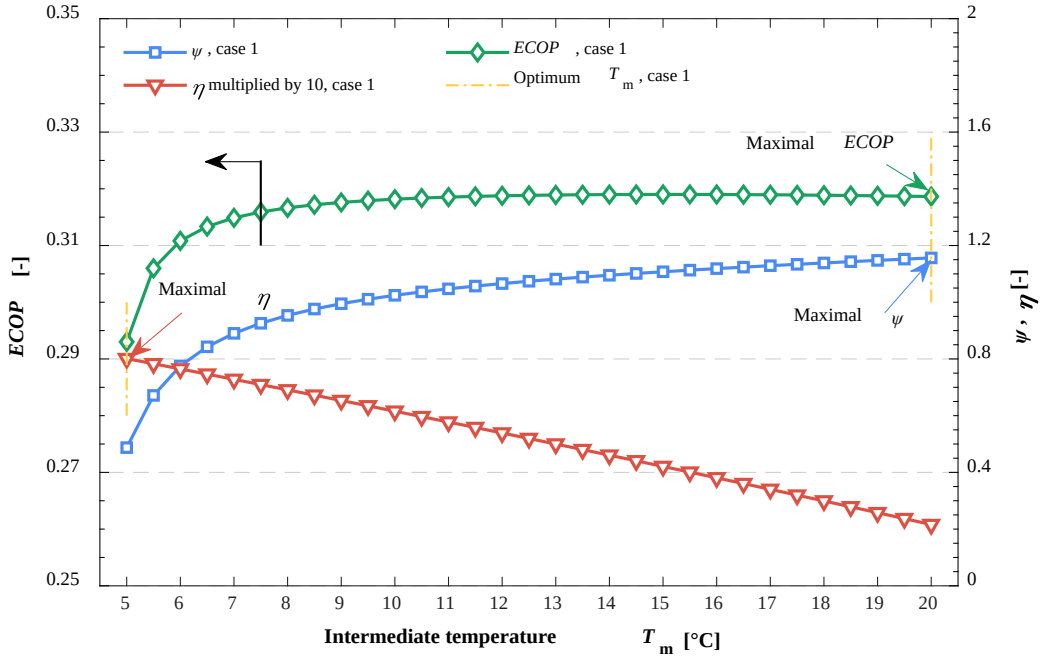

Figure 6. Effect of intermediate temperature on performance indicators for layout with cascade subcooling process in the case 1.

Effect of critical parameters on the performance indicators of solar assisted hybrid cooling systems for case 1 has been shown in Figures 4–6. Note that the duration in heat-driven processes is equal to 1 in this case. It is observed that the different optimum parameters are obtained for various performance indicators. For maximum energy saving factor, it represents that the compressor work consumption of hybrid cooling systems is lowest. Accordingly, lowing the inter-stage pressure and intermediate temperature is beneficial for the compressor work saving. As to maximum exergy efficiency and heat powered coefficient of performance, both are associated with the compressor work and heat exergy consumption, i.e., the summation of compressor work and heat exergy is minimum for the former as well as the compressor work saving to heat exergy is most for the latter.

Table 7. Optimum inter-stage pressures and intermediate temperatures for hybrid cooling systems in the case 1.

System	Optimum critical parameters		
	η	ψ	*ECOP*
TSCTMC	250 kPa	325 kPa	425 kPa
LCC	5 °C	7.5 °C	9 °C
LCS	5 °C	20 °C	20 °C

Optimum inter-stage pressures and intermediate temperatures associated with performance indicators for solar assisted hybrid cooling systems have been listed and compared in Table 7. It is found that the optimal critical parameters corresponding to different performance indicators are significantly different, e.g., the optimum inter-stage pressure ratio of energy saving factor, heat powered coefficient of performance, and exergy efficiency is 1:1.3:1.7.

Preprints (www.preprints.org) | NOT PEER-REVIEWED | Posted: 26 April 2022 doi:10.20944/preprints202204.0229.v1

5.2. System under insufficient heat input

In this section, effect of critical parameters on solar assisted hybrid cooling system performance under insufficient heat input (case 2) is analyzed. Note that the duration in heat-driven processes is less than 1 in this case, and the systems will be degraded into traditional vapor compression cycles when the heat-driven processes are switched off.

Effect of critical parameters on duration in heat-driven processes and compressor work in the case 2 is exhibited in Figures 7–9. There is no doubt that the duration in heat-driven processes enhances with the enhancement of inter-stage pressure or intermediate temperature, owing to the reduction of heat load of generators. Note that the duration in heat-driven processes for layout with cascade condensation process (blue line in Figure 8) tends to be stable with the increase of intermediate temperature, because the *COP* of absorption chiller reaches to plateau and its cooling power almost keeps constant caused by the little variation of latent heat in condensation process. Furthermore, it is observed that the specific drop of compressor work associated with the heat driven process goes down simultaneously. Thereby, the trend of total compressor power is complicated. For two-stage cycle with thermal and mechanical compression processes as well as layout with cascade condensation process, there is an optimum inter-stage pressure and intermediate temperature that minimizes the total compress work, i.e., around 325 kPa and 7.5 °C, which is 61.45% of and close to geometric mean of the evaporator and condenser pressure and temperature, respectively. This is because the lower duration in heat-driven processes impacts the energy saving performance of hybrid cooling systems with lower inter-stage pressure and intermediate temperature. For layout with cascade subcooling process, the compressor work varies slightly with the increase of intermediate temperature. In this regard, it is attributed to that the effect of duration in heat driven processes and that of specific fall in compressor work are nearly offset in arbitrary intermediate temperature.

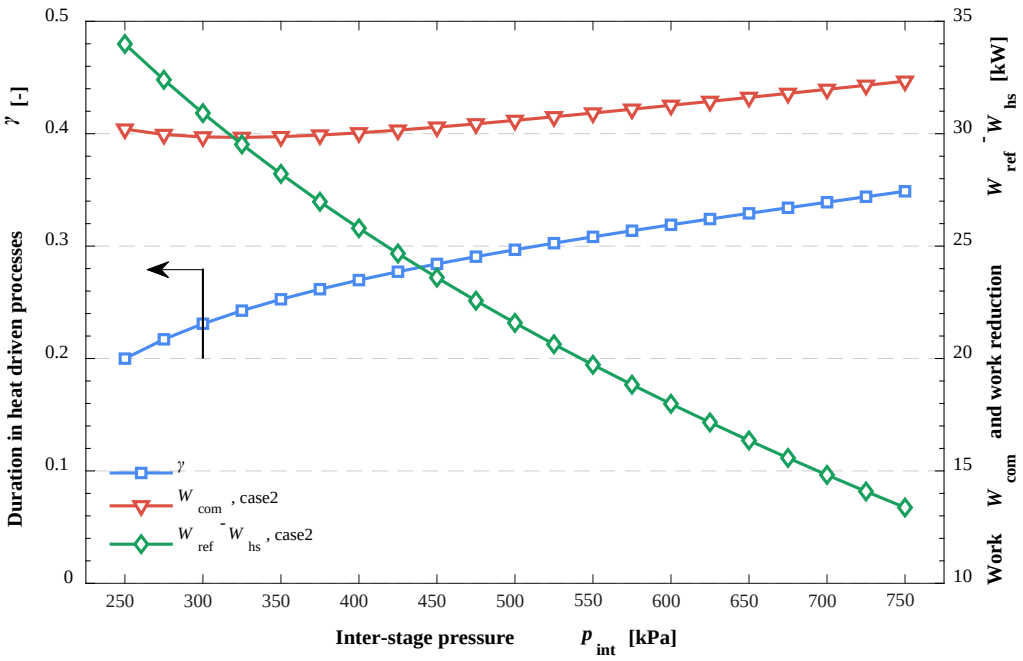

Figure 7. Effect of inter-stage pressure for two-stage cycle with thermal and mechanical compression processes in the case 2.

Preprints (www.preprints.org) | NOT PEER-REVIEWED | Posted: 26 April 2022 doi:10.20944/preprints202204.0229.v1

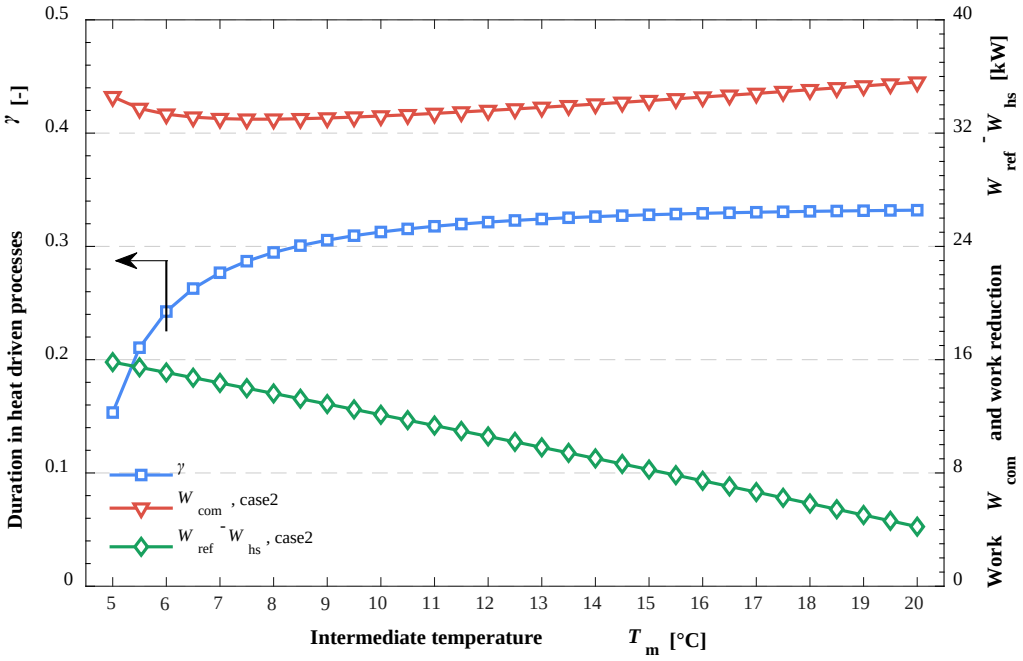

Figure 8. Effect of inter-stage pressure for layout with cascade condensation process in the case 2.

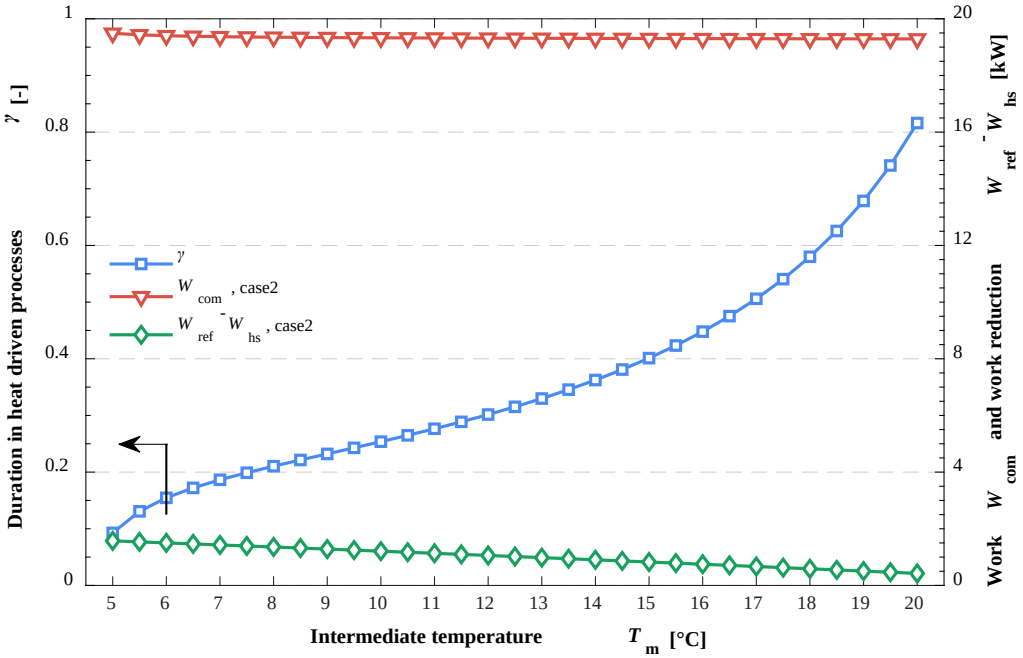

Figure 9. Effect of inter-stage pressure for layout with cascade subcooling process in the case 2.

Preprints (www.preprints.org) | NOT PEER-REVIEWED | Posted: 26 April 2022 doi:10.20944/preprints202204.0229.v1

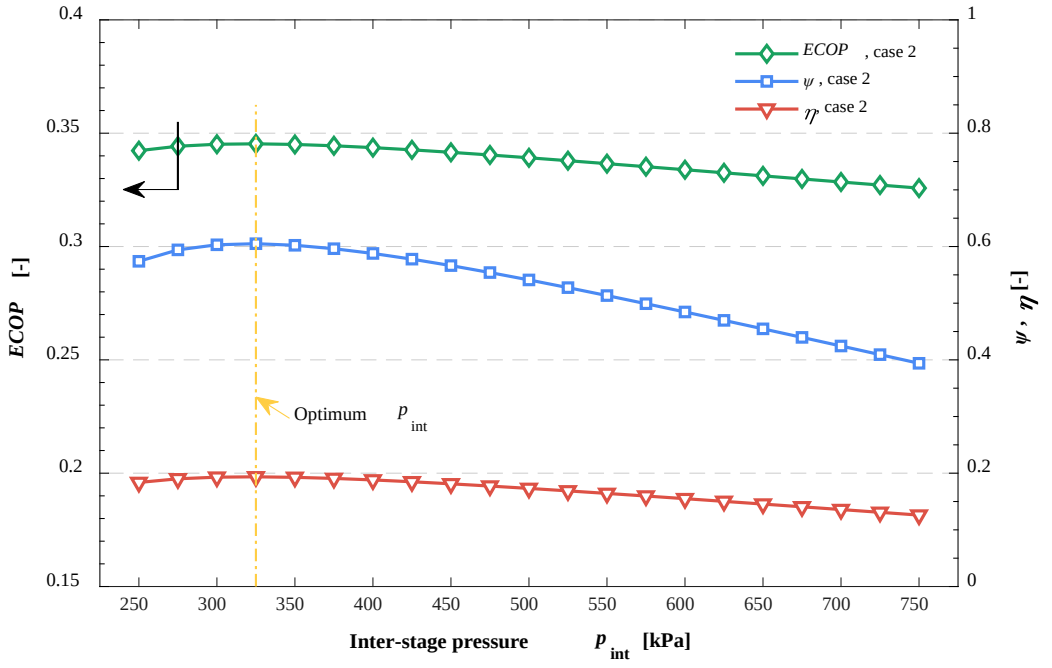

Figure 10. Effect of inter-stage pressure on performance indicators for two-stage cycle with thermal and mechanical compression processes in the case 2.

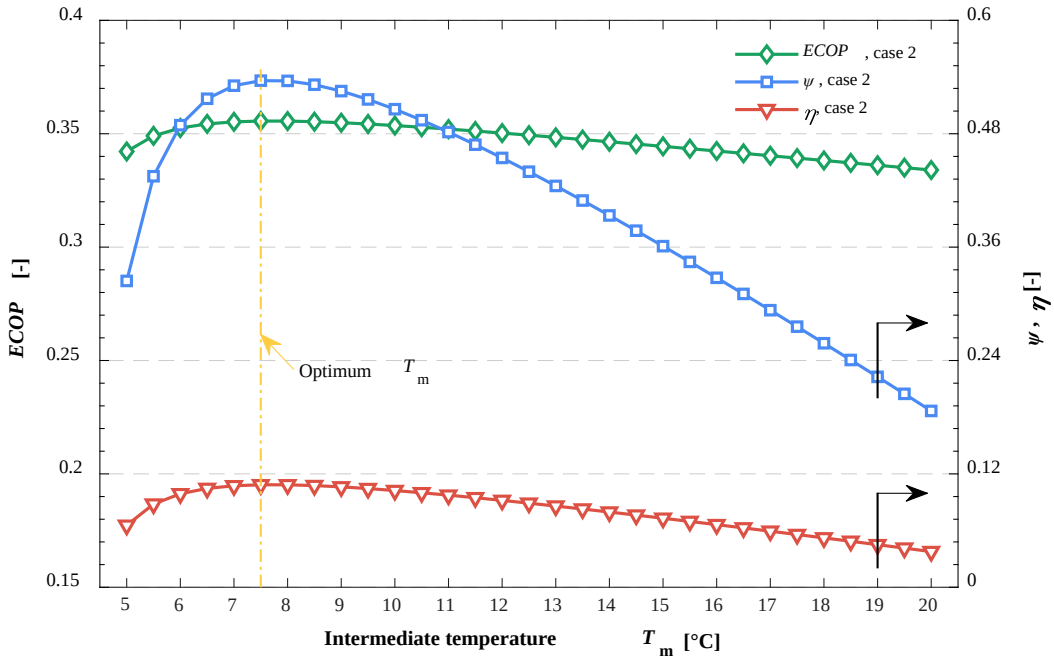

Figure 11. Effect of intermediate temperature on performance indicators for layout with cascade condensation process in the case 2.

Preprints (www.preprints.org) | NOT PEER-REVIEWED | Posted: 26 April 2022 doi:10.20944/preprints202204.0229.v1

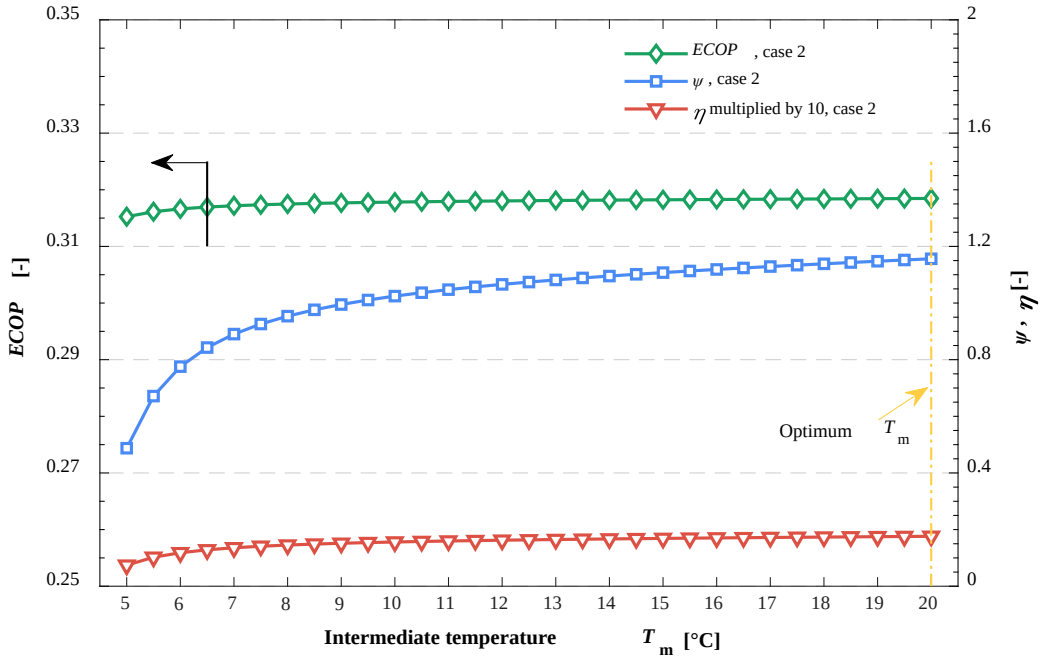

Figure 12. Effect of intermediate temperature on performance indicators for layout with cascade subcooling process in the case2.

Effect of critical parameters on the performance indicators of solar assisted hybrid cooling systems for case 2 is displayed in Figures 10–12. Note that the variation trend of heat powered coefficient of performance is greater than that of exergy efficiency and energy saving factor, which is attributed to the higher reduction of heat exergy consumption. It can be easily known that the performance indicators are related to the compressor work in the case 2 according to Equations (4)–(6). Therefore, performance indicators exhibit the same variation trend, i.e., identical optimum inter-stage pressure as well as intermediate temperature is obtained, when the duration in heat-driven processes has been considered. That is, the optimum inter-stage pressure and intermediate temperature is 61.45% of and close to geometric mean of the evaporator and condenser pressure and temperature, respectively for two-stage cycle with thermal and mechanical compression processes and layout with cascade condensation process. For layout with cascade subcooling process, although the optimum critical parameter is similar to the other two systems, the performance indicators are insensitive to the intermediate temperature from the practical operation viewpoint, i.e., the total compressor work is almost independent of intermediate temperature.

5.3. Optimum parameters for different working conditions

In this section, optimum intermediate temperature as well as inter-stage pressure for different conditions has been discussed in detail. Note that the intermediate temperature has few effects on the performance of layout with cascade subcooling process, thus, the discussion of corresponding layout has been omitted in this section. Moreover, the optimum intermediate temperature and inter-stage pressure have been processed as dimensionless by geometric mean of the evaporator and condenser temperature as well as geometric mean of the evaporator and condenser pressure ($\alpha = T_{\mathrm{m,opt}} \Big/ \sqrt{T_{\mathrm{e}} \cdot T_{\mathrm{c}}}$, $\beta = p_{\mathrm{m,opt}} \Big/ \sqrt{p_{\mathrm{e}} \cdot p_{\mathrm{c}}}$), respectively to make results generally applicable.

Figure 13 displays the effect of inlet temperature of hot water on dimensionless optimum intermediate temperature and inter-stage pressure, respectively for layout with

Preprints (www.preprints.org) | NOT PEER-REVIEWED | Posted: 26 April 2022 doi:10.20944/preprints202204.0229.v1

cascade condensation process and two-stage cycle with thermal and mechanical compression processes. Note that the optimum intermediate temperature for layout with condensation process is close to the geometric mean of the evaporator and condenser temperature (α is almost identical to 1), while the optimum inter-stage pressure is less than the geometric mean of the evaporator and condenser pressure (maximum β is around 0.72). It is found that the optimal critical parameters generally decrease with the enhancement of inlet temperature of hot water, which is attributed to the reduction of the lower limit of evaporator temperature of absorption chiller and absorber pressure of thermal compressor, respectively for layout with cascade condensation process and two-stage cycle with thermal and mechanical compression processes. The dimensionless optimum intermediate temperature is insensitive to the generator temperature for layout with cascade condensation process, i.e., it goes down by 3.47% when the inlet temperature of hot water rises from 70 °C to 90 °C. Note that the optimum intermediate temperature for layout with condensation process keeps constant when the inlet temperature reaches to around 84 °C, because the lower limit of evaporator temperature of LiBr/H_2O absorption chiller cannot be less than 5 °C, owing to the limitation of water solidification temperature. The dimensionless optimum inter-stage pressure for two-stage cycle with thermal and mechanical compression processes is sensitive to the inlet temperature of hot water, i.e., it decreases by 26.67%, with a 20 °C rise in generator temperature.

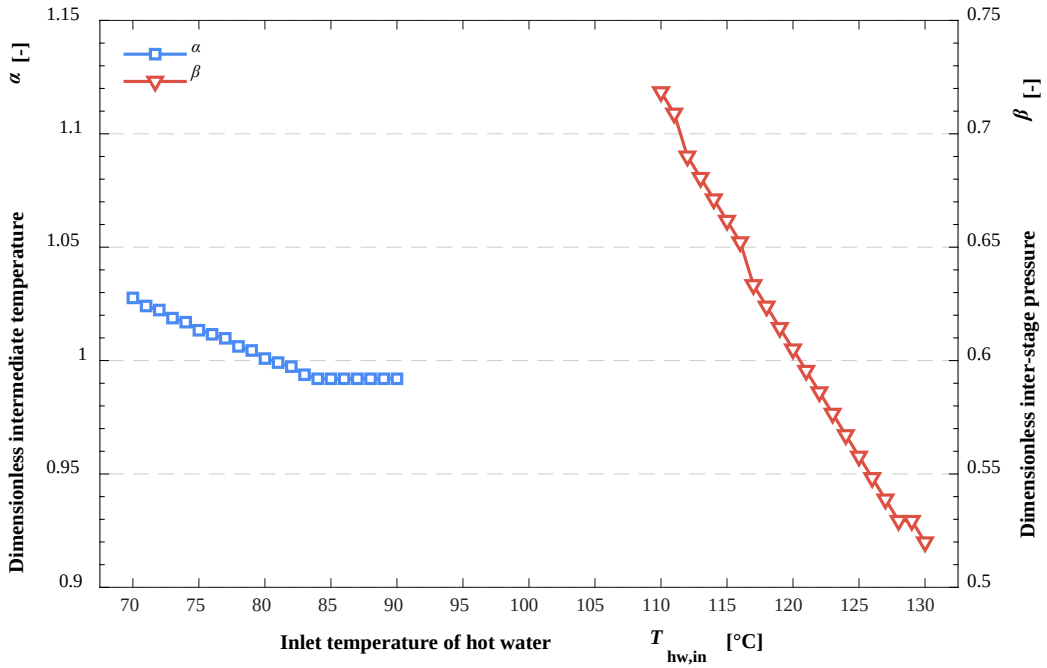

Figure 13. Effect of inlet temperature of hot water on dimensionless optimum intermediate temperature and inter-stage pressure.

Preprints (www.preprints.org) | NOT PEER-REVIEWED | Posted: 26 April 2022 doi:10.20944/preprints202204.0229.v1

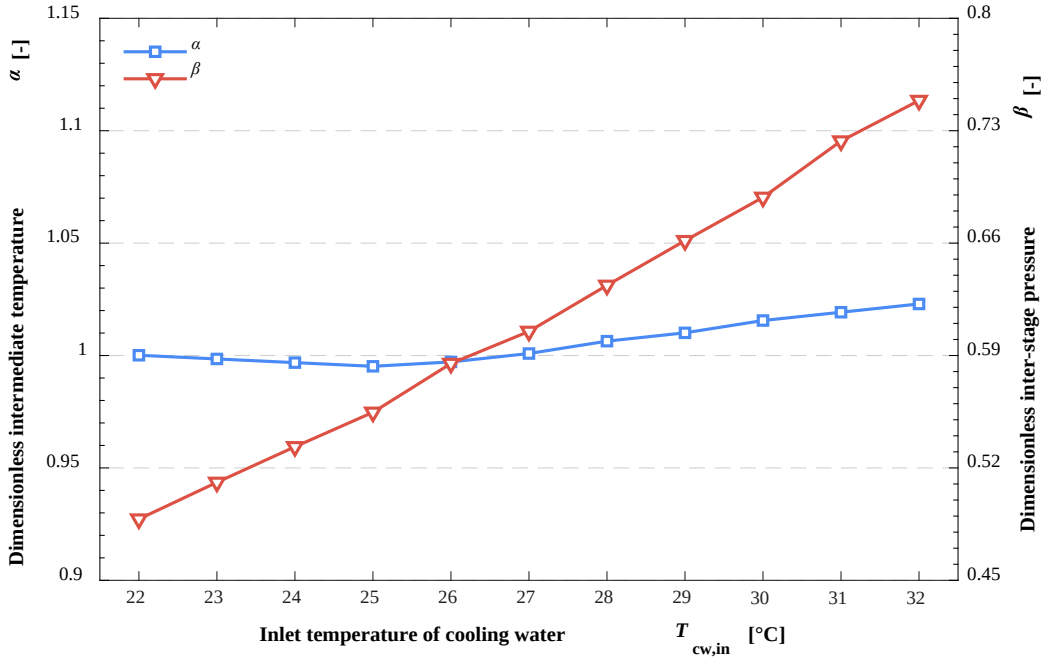

Figure 14. Effect of inlet temperature of cooling water on dimensionless optimum intermediate temperature and inter-stage pressure.

Effect of inlet temperature of cooling water on dimensionless optimum intermediate temperature and inter-stage pressure can be seen in Figure 14. It is noteworthy that the lower limit of evaporator temperature of absorption subsystem for layout with cascade condensation process and absorber pressure of thermal compressor for two-stage cycle with thermal and mechanical compression processes will be enhanced with the growth of inlet temperature of cooling water. Consequently, the optimum inter-stage pressure for two-stage cycle with thermal and mechanical compression processes increases with the rise of inlet temperature of cooling water, i.e., it goes up by 47.27% with a 10 °C rise in condenser temperature. For layout with cascade condensation process, the dimensionless optimum intermediate temperature decreases to a minimum value firstly, and then increases, because the optimum intermediate temperature remains 5 °C (lower limit of evaporator temperature of LiBr/H_2O absorption chiller) while the geometric mean of the evaporator and condenser temperature increases in the case of relatively low condenser temperature. The maximum difference of dimensionless optimum intermediate temperature is around 2.79% with the variation of condenser temperature.

Preprints (www.preprints.org) | NOT PEER-REVIEWED | Posted: 26 April 2022 doi:10.20944/preprints202204.0229.v1

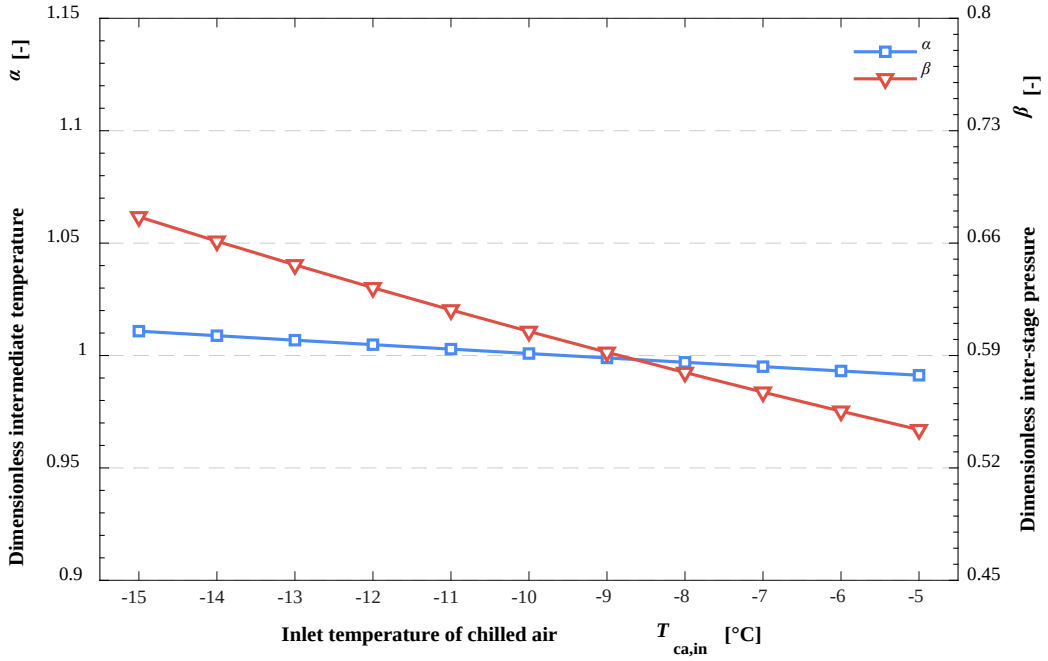

Figure 15. Effect of inlet temperature of chilled air on dimensionless optimum intermediate temperature and inter-stage pressure.

Effect of inlet temperature of chilled air on dimensionless optimum intermediate temperature and inter-stage pressure is exhibited in Figure 15. It is obvious that the variation of inlet temperature of chilled air has no effect on the performance of absorption chiller and thermal compressor, respectively for layout with cascade condensation process and two-stage cycle with thermal and mechanical compression processes. Furthermore, the change of evaporator temperature almost slightly influences the refrigerant flow rate. Namely, the optimum intermediate temperature and inter-stage pressure are constant for corresponding layouts. Note that the decrease in dimensionless optimum intermediate temperature and inter-stage pressure is attributed to the enhancement of geometric mean of the evaporator and condenser temperature and pressure, respectively. The dimensionless optimum intermediate temperature and inter-stage pressure comes down by 1.94% and 24.38%, respectively when the inlet temperature of chilled air grows from -15 °C to -5 °C.

Effect of heat quantity on dimensionless optimum intermediate temperature and inter-stage pressure is shown in Figure 16. It is demonstrated that the optimum intermediate temperature for layout with cascade condensation process as well as optimum inter-stage pressure for two-stage cycle with thermal and mechanical compression processes are independent of the heat quantity. This phenomenon can be exactly illustrated by the results regarding the heat powered coefficient of performance in Section 5.1 (the heat powered coefficient of performance in the case 1 and 2 is coincide). That is, the dimensionless optimum intermediate temperature and inter-stage pressure are dependent on the generator, condenser, absorber, and evaporator temperature.

Preprints (www.preprints.org) | NOT PEER-REVIEWED | Posted: 26 April 2022 doi:10.20944/preprints202204.0229.v1

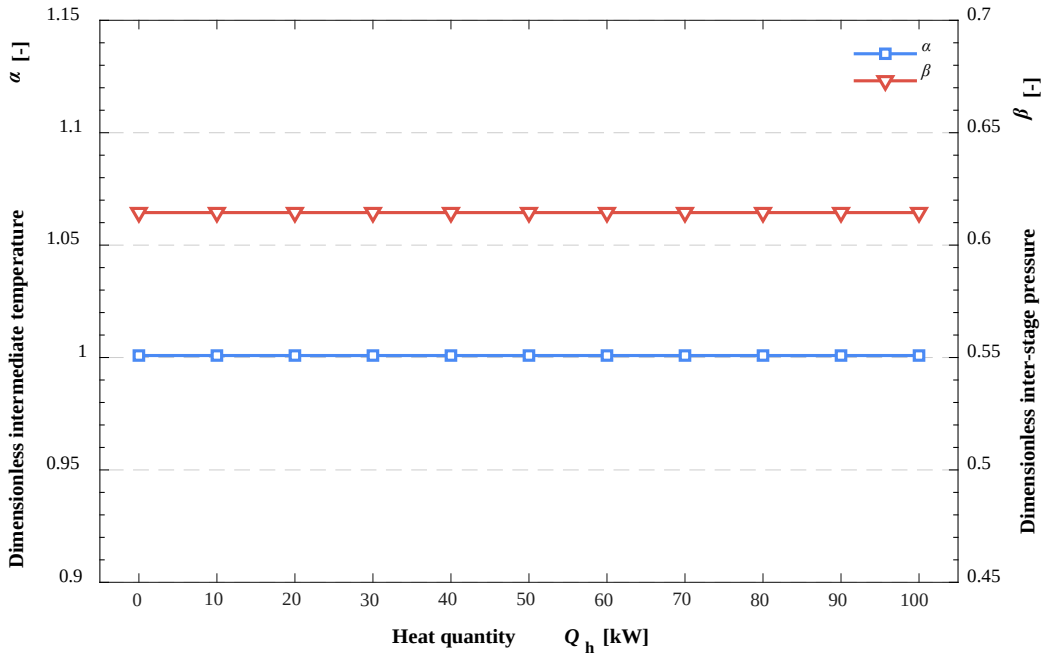

Figure 16. Effect of heat quantity on dimensionless optimum intermediate temperature and inter-stage pressure.=

6. Conclusions

In this study, thermodynamic model of solar assisted hybrid cooling systems with the consideration of duration in heat-driven processes has been established to assess the system performance in entire working periods and applied to three general absorption-compression integrated cycle. The interaction of duration in heat-driven processes and parameters in system performance is discussed. Besides, optimal parameters for different working conditions are obtained. The main conclusions are summarized as follows:

(1) The phenomenon that optimal parameters associated with various performance indicators are conflicting, is corrected by considering the duration of heat-driven processes in the total compressor power, i.e., optimal parameters corresponding to the maximal exergy efficiency, peak heat powered coefficient of performance and the minimal total compressor power are identical.

(2) The dimensionless optimum inter-stage pressure is sensitive to different working conditions for two-stage cycle with thermal and mechanical compression processes. The dimensionless optimum inter-stage pressure goes down by 26.67% and 24.38%, respectively with a 20 °C and 10 °C enhancement in generator and evaporator temperature, while increases by 47.27% when the inlet temperature of cooling water grows from 22 °C to 32 °C.

(3) The dimensionless optimum critical parameter is insensitive to different working conditions for layout with cascade condensation process, i.e., it is close to the geometric mean of the evaporator and condenser temperature. The variation rate of dimensionless optimum intermediate temperature is less than 4% for different working conditions.

(4) The energy saving is almost independent of intermediate temperature for layout with cascade subcooling process, performance indicators are increased slightly with the rise of intermediate temperature.

Author Contributions: Conceptualization, Zeyu Li; Investigation, Zeyu Peng; Methodology, Zeyu Peng; Resources, Zeyu Li; Software, Zeyu Peng and Jianting Yu; Supervision, Zeyu Li; Validation, Junquan Zeng; Writing – original draft, Zeyu Peng; Writing – review & editing, Zeyu Li.

Acknowledgments: This work is supported by: (1) Natural Science Foundation of Guangdong Province under the contract No. 2020B1515120035；2021A1515010265, (2) Fundamental Research Funds for the Central Universities under the contract No. 2020ZYGXZR026, (3) Key Laboratory of Efficient and Clean Energy Utilization of Guangdong Higher Education Institutes under the contract No. KLB10004, (4) Zhuhai Industry-University-Research Cooperation Project under the contract No. ZH22017001210017PWC.

Conflicts of Interest: The authors declare no conflict of interest.

References

1. [1] Soltani M, Dehghani-Sanij A, Sayadnia A, Kashkooli F, Gharali K, Mahbaz S, et al. Investigation of Airflow Patterns in a New Design of Wind Tower with a Wetted Surface. Energies 2018;11:1100.
https://doi.org/10.3390/en11051100
[2] De RK, Ganguly A. Modeling and analysis of a solar thermal-photovoltaic-hydrogen-based hybrid power system for running a standalone cold storage. J Clean Prod 2021;293:126202.
https://doi.org/10.1016/j.jclepro.2021.126202
[3] Zhang N, Lior N, Han W. Performance study and energy saving process analysis of hybrid absorption-compression refrigeration cycles. J Energy Resour Technol 2016;138:061603.
https://doi.org/10.1115/1.4034589
[4] Meng X, Zheng D, Wang J, Li X. Energy saving mechanism analysis of the absorption–compression hybrid refrigeration cycle. Renew Energy 2013;57:43-50.
https://doi.org/10.1016/j.renene.2013.01.008
[5] Wu W, Shi W, Wang B, Li X. Annual performance investigation and economic analysis of heating systems with a compression-assisted air source absorption heat pump. Energy Convers Manage 2015;98:290-302.
https://doi.org/10.1016/j.enconman.2015.03.041
[6] Wu W, Zhang H, You T, Li X. Thermodynamic investigation and comparison of absorption cycles using hydrofluoroolefins and ionic liquid. Industrial & Engineering Chemistry Research 2017;56:9906-16.
https://doi.org/10.1021/acs.iecr.7b02343
[7] Wu W, Shi W, Wang J, Wang B, Li X. Experimental investigation on NH_3–H_2O compression-assisted absorption heat pump (CAHP) for low temperature heating under lower driving sources. Appl Energy 2016;176:258-71.
https://doi.org/10.1016/j.apenergy.2016.04.115
[8] Wang J, Wang B, Li X, Wu W, Shi W. Performance analysis on compression-assisted absorption heat transformer: A new low-temperature heating system with higher heating capacity under lower ambient temperature. Appl Therm Eng 2018;134:419-27.
https://doi.org/10.1016/j.applthermaleng.2018.01.122
[9] Wu W, Wang B, Shang S, Shi W, Li X. Experimental investigation on NH_3–H_2O compression-assisted absorption heat pump (CAHP) for low temperature heating in colder conditions. Int J Refrig 2016;67:109-24.
https://doi.org/10.1016/j.ijrefrig.2016.03.019
[10] Wu W, Wang B, You T, Wang J, Shi W, Li X. Compression-assisted absorption cycles using ammonia and various ionic liquids for cleaner heating. J Clean Prod 2018;195:890-907.
https://doi.org/10.1016/j.jclepro.2018.05.270
[11] Wu W, Leung M, Ding Z, Huang H, Bai Y, Deng L. Comparative analysis of conventional and low-GWP refrigerants with ionic liquid used for compression-assisted absorption cooling cycles. Appl Therm Eng 2020;172:115145.
https://doi.org/10.1016/j.applthermaleng.2020.115145
[12] Liu X, Ye Z, Bai L, He M. Performance comparison of two absorption-compression hybrid refrigeration systems using R1234yf/ionic liquid as working pair. Energy Convers Manage 2019;181:319-30.
https://doi.org/10.1016/j.enconman.2018.12.030
[13] Wu W, You T, Zhang H, Li X. Comparisons of different ionic liquids combined with trans-1,3,3,3-tetrafluoropropene (R1234ze(E)) as absorption working fluids. Int J Refrig 2018;88:45-57.
https://doi.org/10.1016/j.ijrefrig.2017.12.011
[14] Zheng D, Meng X. Ultimate refrigerating conditions, behavior turning and a thermodynamic analysis for absorption–compression hybrid refrigeration cycle. Energy Convers Manage 2012;56:166-74.
https://doi.org/10.1016/j.enconman.2011.10.017
[15] Sun Y, Di G, Wang J, Wang X, Wu W. Performance analysis of R1234yf/ionic liquid working fluids for single-effect and compression-assisted absorption refrigeration systems. Int J Refrig 2020;109:25-36.
https://doi.org/10.1016/j.ijrefrig.2019.10.007
[16] Jain V, Kachhwaha SS, Sachdeva G. Thermodynamic performance analysis of a vapor compression–absorption cascaded refrigeration system. Energy Convers Manage 2013;75:685-700.
https://doi.org/10.1016/j.enconman.2013.08.024
[17] Kairouani L, Nehdi E. Cooling performance and energy saving of a compression–absorption refrigeration system assisted by geothermal energy. Appl Therm Eng 2006;26:288-94.
https://doi.org/10.1016/j.applthermaleng.2005.05.001
[18] He H, Wang L, Yuan J, Wang Z, Fu W, Liang K. Performance evaluation of solar absorption-compression cascade refrigeration system with an integrated air-cooled compression cycle. Energy Convers Manage 2019;201:112153.
https://doi.org/10.1016/j.enconman.2019.112153
[19] Cimsit C. Thermodynamic performance analysis of the double effect absorption-vapour compression cascade refrigeration cycle. J Therm Sci Technol 2018;13:JTST0007.
https://doi.org/10.1299/jtst.2018jtst0007

[20] Sun X, Liu L, Dong Y, Zhuang Y, Zhang L, Du J. Superstructure-based simultaneous optimization of a heat exchanger network and a compression–absorption cascade refrigeration system for heat recovery. Industrial & Engineering Chemistry Research 2020;59:16017-28. https://doi.org/10.1021/acs.iecr.0c02776
[21] Chinnappa JCV, Crees MR, Srinivasa Murthy S, Srinivasan K. Solar-assisted vapor compression/absorption cascaded air-conditioning systems. Sol Energy 1993;50:453-8. https://doi.org/10.1016/0038-092x(93)90068-y
[22] Fernandez-Seara J, Sieres J, Vazquez M. Compression–absorption cascade refrigeration system. Appl Therm Eng 2006;26:502-12. https://doi.org/10.1016/j.applthermaleng.2005.07.015
[23] Garimella S, Brown AM, Nagavarapu AK. Waste heat driven absorption/vapor-compression cascade refrigeration system for megawatt scale, high-flux, low-temperature cooling. Int J Refrig 2011;34:1776-85. https://doi.org/10.1016/j.ijrefrig.2011.05.017
[24] Nagavarapu AK, Garimella S. High-flux thermal management at megawatt scale using a double-effect absorption/vapor-compression cascade refrigeration cycle. Int J Refrig 2020;119:257-67. https://doi.org/10.1016/j.ijrefrig.2020.08.005
[25] Cimsit C, Ozturk IT. Analysis of compression–absorption cascade refrigeration cycles. Appl Therm Eng 2012;40:311-7. https://doi.org/10.1016/j.applthermaleng.2012.02.035
[26] Agarwal S, Arora A, Arora BB. Energy and exergy analysis of vapor compression–triple effect absorption cascade refrigeration system. Eng Sci Technol An Int J 2020;23:625-41. https://doi.org/10.1016/j.jestch.2019.08.001
[27] Jain V, Sachdeva G, Kachhwaha SS. Thermodynamic modelling and parametric study of a low temperature vapour compression-absorption system based on modified Gouy-Stodola equation. Energy 2015;79:407-18. https://doi.org/10.1016/j.energy.2014.11.027
[28] Jain V, Sachdeva GS, Kachhwaha SS. Performance analysis of a vapour compression-absorption cascaded refrigeration system with undersized evaporator and condenser. J Energy S Afr 2014;25:23-36. https://doi.org/10.17159/2413-3051/2014/v25i4a2234
[29] Salhi K, Korichi M, Ramadan KM. Thermodynamic and thermo-economic analysis of compression–absorption cascade refrigeration system using low-GWP HFO refrigerant powered by geothermal energy. Int J Refrig 2018;94:214-29. https://doi.org/10.1016/j.ijrefrig.2018.03.017
[30] Colorado D, Rivera W. Performance comparison between a conventional vapor compression and compression-absorption single-stage and double-stage systems used for refrigeration. Appl Therm Eng 2015;87:273-85. https://doi.org/10.1016/j.applthermaleng.2015.05.029
[31] Liu L, Li Z, Jing Y, Lv S. Energetic, economic and environmental study of cooling capacity for absorption subsystem in solar absorption-subcooled compression hybrid cooling system based on data of entire working period. Energy Convers Manage 2018;167:165-75. https://doi.org/10.1016/j.enconman.2018.04.102
[32] Salajeghe M, Ameri M. Energy and exergy analysis of subcooling the condenser outlet refrigerant in a compression-absorption cascade refrigeration system. Int J Exergy 2015;18:234-50. https://doi.org/10.1504/Ijex.2015.072170
[33] Jain V, Colorado D. Thermoeconomic and feasibility analysis of novel transcritical vapor compression-absorption integrated refrigeration system. Energy Convers Manage 2020;224:113344. https://doi.org/10.1016/j.enconman.2020.113344
[34] Li Z, Chen E, Jing Y, Lv S. Thermodynamic relationship of subcooling power and increase of cooling output in vapour compression chiller. Energy Convers Manage 2017;149:254-62. https://doi.org/10.1016/j.enconman.2017.07.030
[35] Chen E, Li Z, Yu J, Xu Y, Yu Y. Experimental research of increased cooling output by dedicated subcooling. Appl Therm Eng 2019;154:9-17. https://doi.org/10.1016/j.applthermaleng.2019.03.071
[36] He L, Wang S, Liu S, Xuan W. Numerical and experimental evaluation of the performance of a coupled vapour absorption-compression refrigeration configuration. Int J Refrig 2019;99:429-39. https://doi.org/10.1016/j.ijrefrig.2018.11.023
[37] Yu J, Li Z, Chen E, Xu Y, Chen H, Wang L. Experimental assessment of solar absorption-subcooled compression hybrid cooling system. Sol Energy 2019;185:245-54. https://doi.org/10.1016/j.solener.2019.04.055
[38] Xu Y, Li Z, Chen H, Lv S. Techno-economic evaluation and analysis of solar hybrid cooling systems with cool energy buffer for cold storages. Sustainable Energy Technologies and Assessments 2021;46:101270. https://doi.org/10.1016/j.seta.2021.101270
[39] Xu Y, Jiang N, Pan F, Wang Q, Gao Z, Chen G. Comparative study on two low-grade heat driven absorption-compression refrigeration cycles based on energy, exergy, economic and environmental (4E) analyses. Energy Convers Manage 2017;133:535-47. https://doi.org/10.1016/j.enconman.2016.10.073
[40] Sun L, Han W, Jin H. Energy and exergy investigation of a hybrid refrigeration system activated by mid/low-temperature heat source. Appl Therm Eng 2015;91:913-23. https://doi.org/10.1016/j.applthermaleng.2015.08.061
[41] Avanessian T, Ameri M. Energy, exergy, and economic analysis of single and double effect LiBr–H_2O absorption chillers. Energy Build 2014;73:26-36. https://doi.org/10.1016/j.enbuild.2014.01.013
[42] Li Z, Jing Y, Liu J. Thermodynamic study of a novel solar LiBr/H_2O absorption chiller. Energy Build 2016;133:565-76. https://doi.org/10.1016/j.enbuild.2016.10.022
[43] Xu Y, Jiang N, Wang Q, Chen G. Comparative study on the energy performance of two different absorption-compression refrigeration cycles driven by low-grade heat. Appl Therm Eng 2016;106:33-41. https://doi.org/10.1016/j.applthermaleng.2016.05.169
[44] Lecuona A, Ventas R, Venegas M, Zacarías A, Salgado R. Optimum hot water temperature for absorption solar cooling. Sol Energy 2009;83:1806-14.

https://doi.org/10.1016/j.solener.2009.06.016
[45] Peng Z, Li Z, Zeng J, Xu Y. Differences of energy saving quantities for absorption-compression hybrid cooling systems with cascade condenser and cascade subcooler. Int J Energy Res 2021;45:19439-52.
https://doi.org/10.1002/er.7033
[46] Patek J, Klomfar J. A computationally effective formulation of the thermodynamic properties of LiBr–H_2O solutions from 273 to 500K over full composition range. Int J Refrig 2006;29:566-78.
https://doi.org/10.1016/j.ijrefrig.2005.10.007